

DFNE 22-XXXX



Multiple Continuum Approach to Modeling Radionuclide Transport in Fractured Networks

Leone, R.C. and Nole, M.

Sandia National Laboratories, Albuquerque, NM, USA

Hammond, G.E.

Pacific Northwest National Laboratory, Richland, WA, USA

Lichtner, P.C.

University of New Mexico, Albuquerque, NM, USA

Copyright © 2022 DFNE, ARMA

This paper was prepared for presentation at the 3rd International Discrete Fracture Network Engineering Conference held in Santa Fe, New Mexico, USA, June 29-July 1, 2022. This paper was selected for presentation at the symposium by the DFNE Technical Program Committee based on a technical and critical review of the paper by a minimum of two technical reviewers. The material, as presented, does not necessarily reflect any position of ARMA, its officers, or members. Electronic reproduction, distribution, or storage of any part of this paper for commercial purposes without the written consent of ARMA/DFNE is prohibited. Permission to reproduce in print is restricted to an abstract of not more than 200 words; illustrations

ABSTRACT: Traditional discrete fracture models implementing matrix diffusion can be computationally expensive and only applicable to simplified transport problems. Upscaling to a continuum model can reduce computational burden, but models based on only a primary continuum neglect fracture-matrix interaction. PFLOTRAN, a subsurface flow and reactive transport code, simulates a secondary continuum (matrix) coupled to the primary continuum (fracture) modeled as a disconnected one-dimensional domain using a method known as the Dual Continuum Disconnected Matrix (DCDM) model. This work presents several benchmarks to compare PFLOTRAN's DCDM model to analytical solutions and a large-scale test problem in a one cubic km fractured domain modeling a conservative tracer with diffusion of the tracer into the rock matrix. The tracer was modeled using two different methods: first, with a Discrete Fracture Network (DFN) representation, and second, using the DCDM in PFLOTRAN. We find that the DCDM representation of the upscaled fracture network produces results comparable to the DFN and analytical solutions where available, verifying this method. We then apply the DCDM model to a fractured domain considering radionuclide isotope sorption, partitioning, decay, and ingrowth and find that radionuclide retardation is enhanced when considering these additional mechanisms.

1. INTRODUCTION

Matrix diffusion coupled with sorption is currently considered one of the most important radionuclide retardation mechanisms in fractured crystalline host rock (SKBF 1983). One way of modeling diffusive transport between a rock matrix and fractures is by representing the phenomenon as a Fickian diffusion process over a dual porosity (dual continuum) system. This stands in contrast to traditional discrete fracture models used to simulate matrix diffusion, which can be computationally expensive due to the need for fine meshes and are applicable only to simplified solute transport problems. Upscaling to a continuum model can reduce computational burden, but models based on only a single continuum neglect fracture-matrix interaction.

PFLOTRAN, a subsurface flow and reactive transport code, simulates a secondary continuum (matrix) coupled to the primary continuum (fracture) modeled as a disconnected one-dimensional domain using a method known as the Dual Continuum Disconnected Matrix (DCDM) model (Lichtner, 2000). Since secondary continua are isolated from one another, the formulation

for the secondary continuum equations is embarrassingly parallel, making PFLOTRAN's DCDM model ideal for complex full-scale crystalline repositories using high performance computing. In this work, we test PFLOTRAN's DCDM model to represent fracture-matrix interactions against several analytical solutions and benchmarks and then apply the model to a problem considering radionuclide transport in a large-scale fractured rock domain.

2. MODELING APPROACH

The DCDM model in PFLOTRAN solves equations for a primary and secondary continuum in a fully coupled implementation. The primary continuum is modeled via (Eq. 1):

$$\begin{aligned} \frac{\partial}{\partial t} (\epsilon_f \varphi_f \Psi_j^f) + \nabla \cdot \Omega_j^f = & - A_{fm} \Omega_j^{fm} \\ & - \epsilon_f \sum_k \nu_{jk} \Gamma_k^f - \epsilon_f \frac{\partial S_j^f}{\partial t} \end{aligned} \quad \#(1)$$

where f and m denote the fracture and matrix continua, respectively, ϵ_f is the fracture volume fraction, φ is porosity, ψ_j^f is the total component concentration (includes aqueous complexes) in the fracture of species j , Ω_j^f is total solute flux in the fracture, Ω_j^{fm} is total solute flux between the fracture and matrix, A_{fm} is the fracture-matrix interfacial area, v_{jk} is the stoichiometric coefficient, Γ_k^f is the mineral reaction, and S_j^f is the sorption isotherm. Advection and dispersion are allowed in the primary continuum, and in the secondary continuum transport occurs through diffusion only. The secondary continuum is modeled as a one-dimensional domain where diffusive fluxes occur perpendicular to the fracture wall (Eq. 2):

$$\frac{\partial}{\partial t}(\varphi_m \psi_j^m) + \nabla_\xi \cdot \Omega_j^m = - \sum_k v_{jk} \Gamma_k^m - \frac{\partial S_j^m}{\partial t} \quad \#(2)$$

where the gradient operator ∇_ξ refers to the effective one-dimensional secondary continuum geometry. Each primary continuum cell has a corresponding set of secondary continuum cells attached to it. The secondary cells cannot interact with secondary cells associated with other primary cells. The equations for the primary and secondary continuum are solved separately and coupled together by the mass exchange flux (Eq. 3) assuming symmetry along the axis dividing them (Iraola et al., 2019):

$$\Omega_j^{fm}(x,t) = \Omega_j^m(\xi_{fm}, x \mid r) \quad \#(3)$$

where x is a point in the primary continuum, t is time and ξ_{fm} is the outer boundary of the secondary continuum. In this approach a backward solve is first performed on the secondary continuum to eliminate coupling to the fracture, followed by solving the primary continuum equations (Lichtner and Karra, 2014). The solution is completed with a forward solve of the secondary continuum. This contrasts with the Multiple Interacting Continua (MINC) dual continuum approach used in the flow and reactive transport simulator TOUGH, where the secondary and primary are treated as a single system solved simultaneously. Since the primary and secondary continua are decoupled, this makes the DCDM approach in PFLOTRAN ideal for complex and challenging transport problems.

3. BENCHMARK RESULTS

Several different benchmark problems were performed to validate the DCDM model in PFLOTRAN.

3.1. Tang et al., 1981

The first benchmark test is based on the analytical solution by Tang et al., 1981 for the problem of transport

of a radionuclide in a single fixed-aperture fracture with diffusion into the rock matrix, where the rock matrix is assumed to be infinite. Parameters used for this comparison can be found in Table 1. A Dirichlet boundary condition was assumed at the inlet and modeled to 10,000 days. 100 cells were used to model the primary continuum where each cell had 100 secondary cells. Normalized concentration along the fracture and concentration into the matrix at 100, 1,000, and 10,000 days can be seen in Figure 1 where the DCDM model shows excellent agreement with the analytical solution in the fracture and matrix.

Table 1. Parameters used for Tang et al., 1981 benchmark

Parameter	Value
Diffusion coefficient in water	$1.6 \times 10^{-9} \text{ m}^2/\text{s}$
Tortuosity	0.1
Fracture width	10^{-4} m
Dispersivity	0.5 m
Half-life	12.35 y
Retardation factor in matrix (R')	1.0
Retardation factor in fracture	1.0
Matrix Porosity	0.01
Concentration, ($z=0$)	1.0 M
Average linear velocity in fracture	0.01 m/d

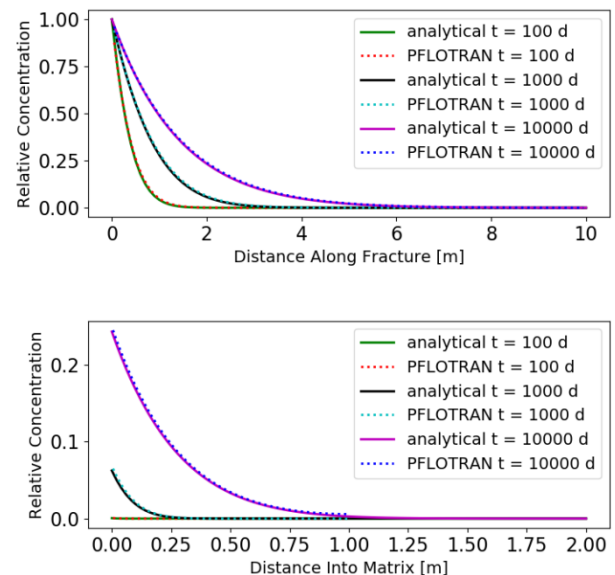


Fig. 1. Comparisons for concentration along fracture (top) and into the matrix (bottom) at $z = 2$ m down fracture.

This benchmark case was then expanded to test retardation factors in the matrix (R') of 2, 5, and 10. The results can be seen in Figure 2 at a time of 1,000 days.

These comparisons expand on Iraola et al., 2019 by adding in dispersion and retardation in the fracture and matrix.

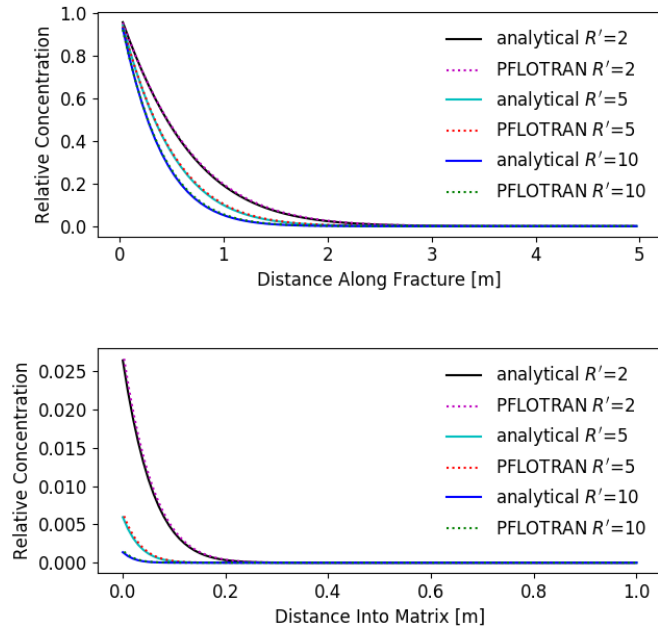


Fig. 2. Comparisons at 1,000 days for various retardation factor along the fracture (top) and into the matrix (bottom) at a location of 2 m down the fracture.

3.2. Sudicky and Frind, 1982

The work by Sudicky and Frind, 1982 describes an extension of Tang et al., 1981 of transport in discrete parallel fractures connected to a finite matrix domain. A benchmark case was developed using the same parameters in Table 1, but with two different finite matrix lengths. A small matrix size of 0.05 m and a larger matrix of 0.25 m were tested. The results are shown in Figure 3, where observation points are plotted along distances of 1, 2, and 3 m down the fracture.

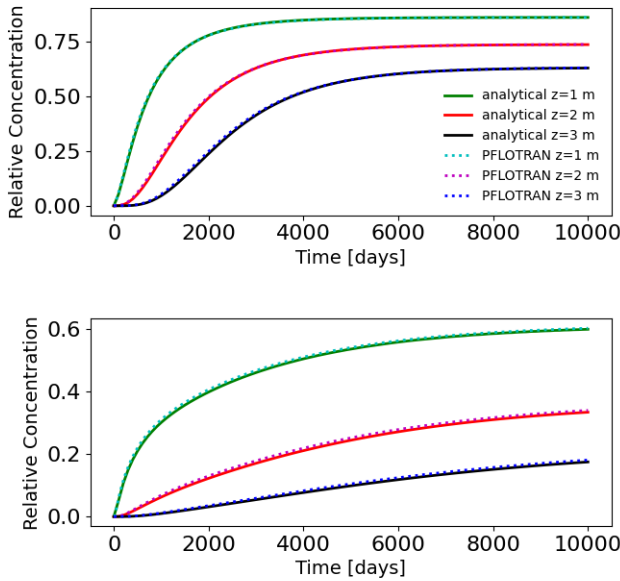


Fig. 3. Breakthrough curves for small matrix of 0.05 m (top) and large matrix size of 0.25 m (bottom). Z values represent meters down the fracture. Solid lines represent the analytical solution and dotted lines represent the PFLOTRAN solution.

3.3. 4-Fracture DFN

A four-fracture test problem was developed to demonstrate the capability in PFLOTRAN's DCDM model of defining spatially varying fracture properties across a domain. The problem (built based on an example provided with dfnWorks [Hyman et al., 2015]) models advection and diffusion of a conservative tracer through four fractures within a cubic domain with diffusion into the rock matrix. Groundwater flow is simulated by a steady (saturated, single-phase) pressure gradient along the x-axis (Figure 4). Constant pressure (Dirichlet) boundary conditions were applied on the inflow and outflow faces. An initial pulse of tracer was inserted uniformly along the fractures on the west face ($x = -500$) of the domain at time zero; the concentration at the west face was set to zero for all other times. The tracer exits the domain through the fractures on the east face ($x = 500$). All other faces were assigned no flow boundary conditions. Diffusion into the matrix occurs along the fractures.

Table 2. Parameters used for four-fracture benchmark.

Parameter	Value
Pressure (inlet $x = -500$)	1.001×10^6 Pa
Pressure (outlet, $x = 500$)	1.0×10^6 Pa
Porosity in fracture	1.0
Tortuosity in fracture	1.0
Matrix porosity	0.005
Matrix permeability	10^{-18} m ²
Matrix diffusion coefficient	1.6×10^{-10} m ² /s
ECPM cell size	20 m

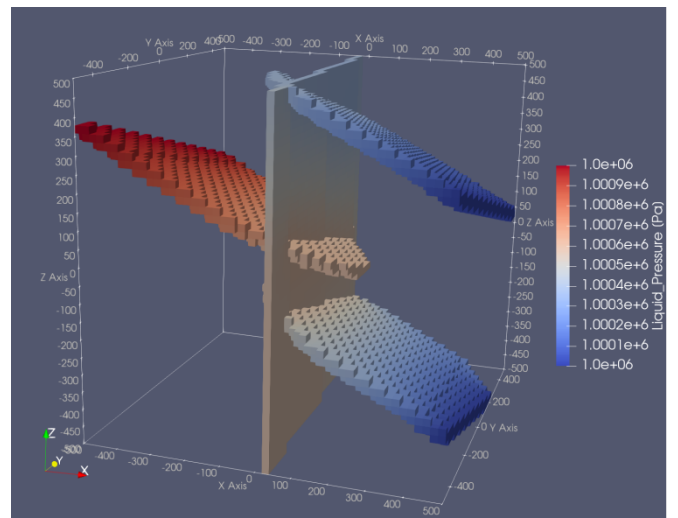


Fig. 4a. Four-fracture pressure solution for ECPM

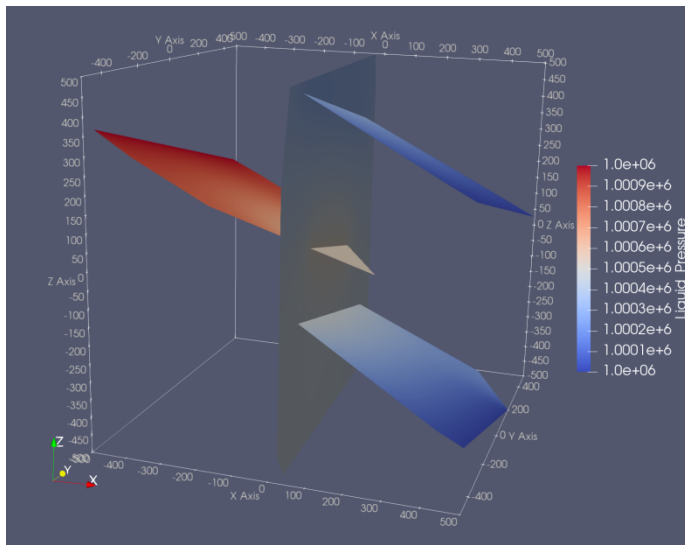


Fig. 4b. Four-fracture pressure solution for DFN

The tracer was modeled using two different methods. The first method used LANL dfnTrans particle tracking software (Lagrangian reference frame). Matrix diffusion is simulated via a time domain random walk approach and Darcy velocities were calculated from the DFN steady state flow solution simulated in PFLOTRAN. The second method used PFLOTRAN's reactive transport mode (Eulerian reference frame) with the DCDM model. To simulate transport in PFLOTRAN, the fractures were upscaled to an Equivalent Continuous Porous Medium (ECPM) via a Python script mapDFN (Stein et al., 2017). dfnWorks outputs apertures, permeabilities, radii, the vector defining the unit normal to the fractures, and coordinates of the fracture center. These files along with parameters defining the domain and grid cell size for the ECPM were used as input for mapDFN. Upscaled anisotropic permeability, porosity, and tortuosity were then outputted based on the intersection of fractures within grid cells. The porosity values for the ECPM were then used as input into the DCDM model to define fracture volume fraction. The matrix length for each grid cell was specified as (1 – porosity in grid cell) x 20 m.

Normalized breakthrough curves (total mass that has crossed the east face divided by the initial mass at the west face) were generated at the outflow face (Figure 5). Both transport methods were also applied on the system without matrix diffusion. The DCDM model and DFN show comparable results. The models with and without matrix diffusion show similar results at the beginning of the simulation and then verge at later times as tracer diffuses into the rock matrix. Differences in results may be due to grid discretization, upscaling methods and fracture characterization. The DCDM modeled in

PFLOTRAN may also experience more numerical dispersion than the DFN particle tracking results.

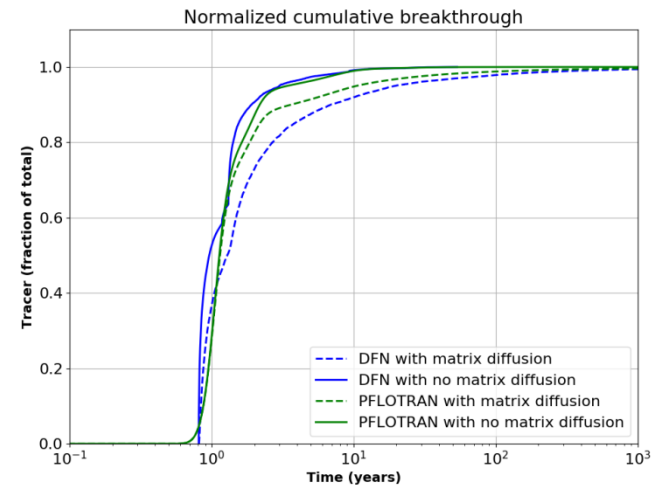


Fig. 5. Breakthrough curves for 4-Fracture Benchmark

3.4. 4-Fracture plus Stochastic Fractures DFN

The four-fracture benchmark case was expanded on by adding stochastic fractures in the domain. The stochastic fractures were generated based on Central Hydraulic Unit West (CHUW) Case A distributions from Posiva WR 2012-42 (Hartley et al., 2013, Table D-4) corresponding to Depth Zone 4, which applies at repository depth (Hartley et al., 2016, Table 3-1). Figures 6 shows the steady-state fracture domain pressure solution used for the transport simulations.

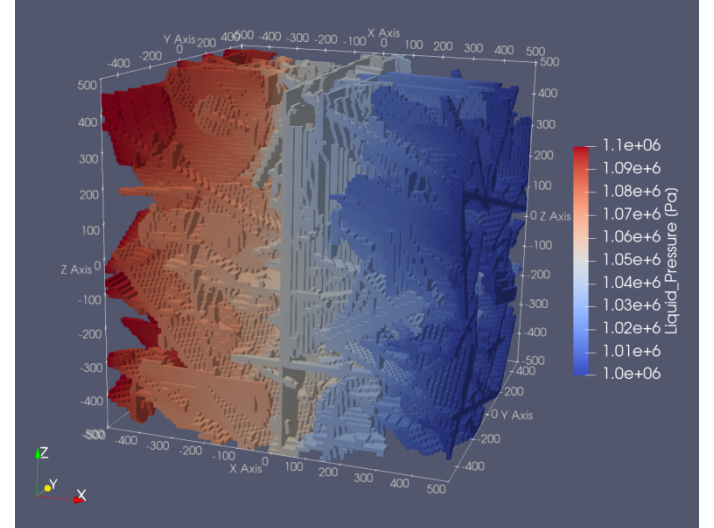


Fig. 6a. Four-fracture plus stochastic fractures pressure solution for the ECPM.

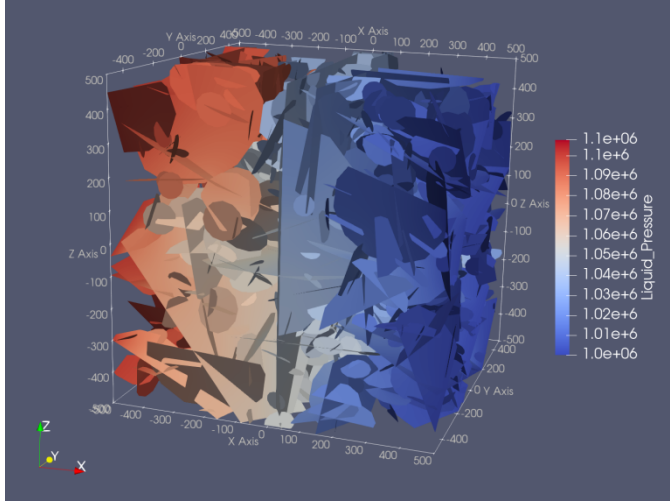


Fig. 6b. Four-fracture pressure solution plus stochastic fractures for DFN

Table 3 shows material and fluid properties that were altered in the model from the four-fracture case to reduce breakthrough time. Breakthrough curves generated at the outflow (east face) for the two methods were plotted over 1,000,000 years (Figure 7). The results again show comparable results with similar breakthrough times. In this scenario, the addition of matrix diffusion significantly retards the tracer and breakthrough occurs much later. In the simulations with matrix diffusion the DFN shows breakthrough first but then takes longer than 1,000,000 years for all particles to pass through.

Table 3. Four-fracture plus stochastic fractures parameter values

Parameter	Value
Pressure (inlet $x = -500$)	1.1×10^6 Pa
Pressure (outlet, $x = 500$)	1.0×10^6 Pa
Matrix diffusion coefficient	1.6×10^{-12} m ² /s

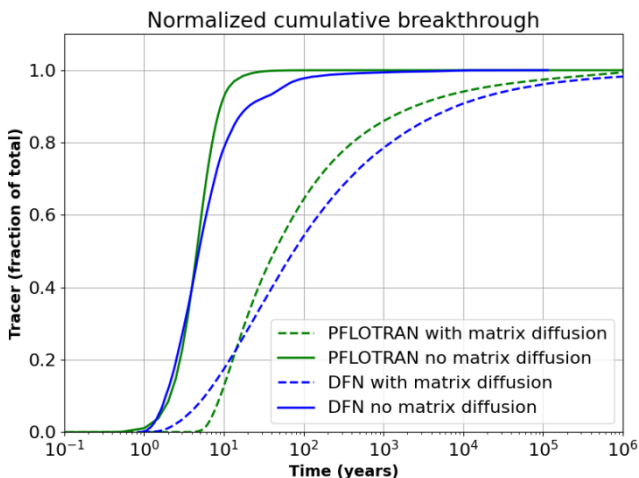


Fig. 7. Breakthrough curves for four-fracture plus stochastic fractures with and without matrix diffusion

4. UFD DECAY

The Used Fuel Disposition (UFD) Decay Process Model in PFLOTRAN models radionuclide isotope decay, ingrowth, and phase partitioning and was created for use as part of the Geologic Disposal Safety Assessment (GDSA) Framework. The model is called at each transport time step where the total mass of each isotope is summed based on the mass in the aqueous, sorbed, and precipitated phase. The total mass then decays according to the Bateman Equations. Afterwards, the total mass is partitioned back into aqueous, sorbed, and precipitated phases and isotope concentrations are calculated from the isotope mole fraction and elemental concentrations.

A single decay chain was modeled using the UFD decay model and applied to the single fracture problem considering the isotope ^{241}Am decaying to ^{237}Np versus a non-decaying tracer diffusing into the matrix. Solubility, distribution coefficients, and decay rates were taken from Mariner et al., 2011 and are listed in Table 4.

Table 4. UFD Decay test problem values

Parameter	Value
Inlet concentration ^{241}Am	4×10^{-7} mol/kg
Inlet concentration ^{237}Np	1×10^{-12} mol/kg
^{241}Am Solubility	4×10^{-7} mol/L
^{237}Np Solubility	4×10^{-9} mol/L
^{241}Am Matrix K_d	0.04 m ³ /kg
^{237}Np Matrix K_d	0.2 m ³ /kg
^{241}Am Decay Rate	5.08×10^{-11} 1/s
^{237}Np Decay Rate	1.03×10^{-14} 1/s

The concentration in the fracture and matrix can be seen in Figure 8 and 9 respectively at 1,000 and 5,000 days. Tracer can be seen as far as ~ 4 m at 5,000 days in the non-decaying tracer scenario. In the decaying isotope scenario, the isotope travels less than 2 m down the fracture at 5,000 days. The results show increase in radionuclide retardation when considering decay in a fractured system.

The test problem was then applied to the 4-fracture network considering an inlet pulse of ^{241}Am decaying to ^{237}Np . Figure 10 shows the mean concentration of each isotope in the entire system and Figure 11 shows moles of each isotope passing through the outflow boundary ($x = 500$ m) with time. The mean concentration of ^{237}Np increases once ^{241}Am decays and then decreases again around $\sim 1,000$ years.

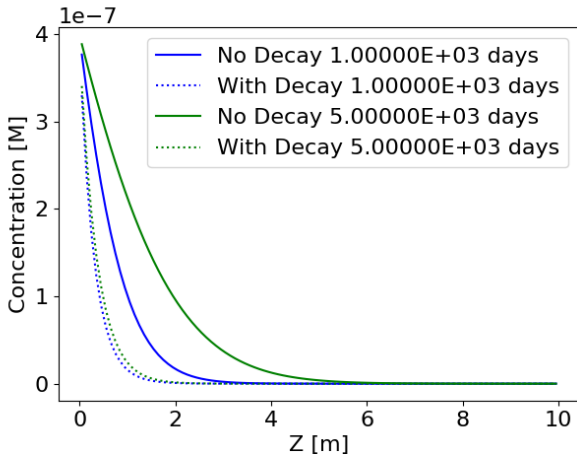


Fig. 8. Concentration in the fracture with a decaying isotope (dotted line) versus non decaying tracer (solid line)

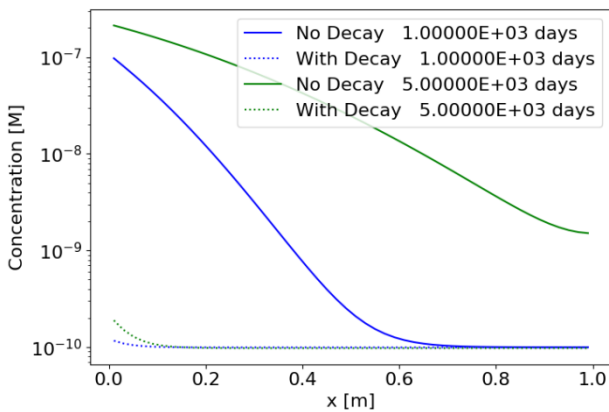


Fig. 9. Concentration in the matrix with a decaying isotope (dotted line) versus non decaying tracer (single line)

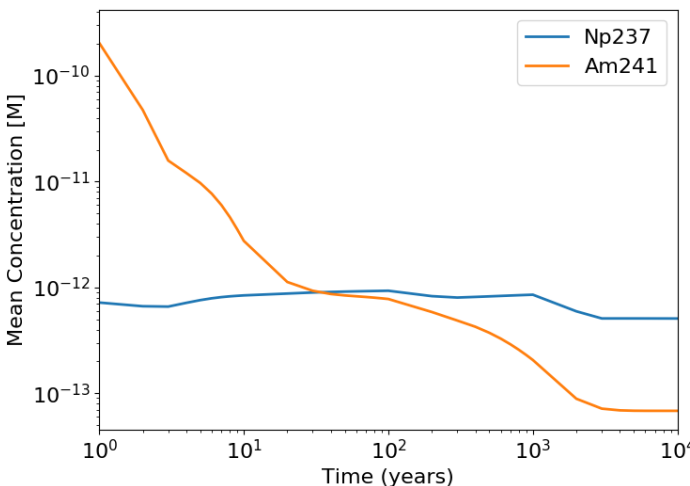


Fig. 10. Mean concentration of isotopes in the entire system

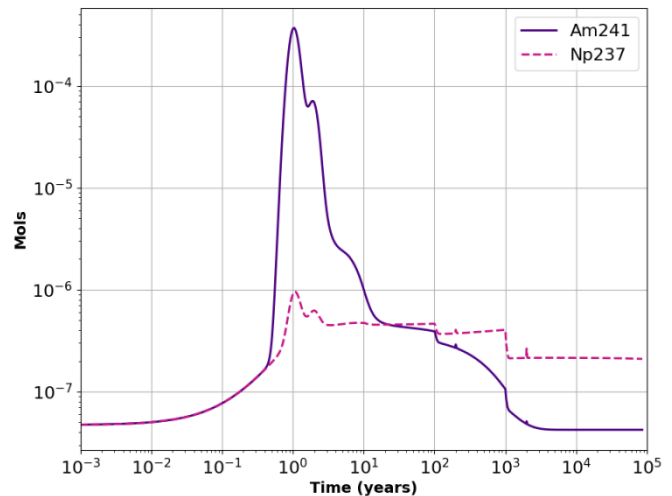


Fig. 11. Moles of each isotope passing through outflow

5. CONCLUSIONS

The DCDM model in PFLOTRAN allows for representation of fracture-matrix interactions in large scaled fractured rock, and it has recently been updated to model advanced radionuclide transport via the UFD Decay process model. In this work, we present verification of the multiple continuum model in PFLOTRAN against two single-fracture analytical solutions and a numerical DFN particle tracking example in several multi-fracture domains. The DCDM model in PFLOTRAN produces results comparable to the DFN particle tracking, while allowing for advanced solute transport. Furthermore, the tests demonstrate that matrix diffusion can in fact have a significant impact on solute transport simulations.

astly, a test case was developed considering radionuclide isotope sorption, partitioning, and decay of two different isotopes. This analysis demonstrates the ability of PFLOTRAN's DCDM model to be used as part of a full-scale performance assessment of a deep geological repository in fractured crystalline rock.

ACKNOWLEDGEMENTS

Thank you to the members of DECOVALEX-2023 Task for help in designing the single fracture, 4-fracture, and -fracture plus stochastic fractures benchmark tests.

Sandia National Laboratories is a multi-mission laboratory managed and operated by National Technology and Engineering Solutions of Sandia LLC, a wholly-owned subsidiary of Honeywell International Inc. for the U.S. Department of Energy's National Nuclear Security Administration under contract DE-NA0003525.

REFERENCES

1. Hazzard, J.F., R.P. Young, and S.C. Maxwell. 2000. Micromechanical modeling of cracking and failure in brittle rocks. *J. Geophys. Res.* 105: 16,683–16,697.
2. Hartley, L., J. Hoek, D. Swan, P. Appleyard, S. Baxter, D. Roberts, and T. Simpson. 2013. *Hydrogeological Modelling for Assessment of Radionuclide Release Scenarios for the Repository System 2012*. Working Report 2012-42. Posiva Oy.
3. Hartley, L., S. Baxter, and T. Williams 2016. *Geomechanical Coupled Flow in Fractures during Temperate and Glacial Conditions*. Working Report 2016-08. Posiva Oy, Eurajoki, Finland.
4. Iraola, A., P. Trinchero, S. Karra and J. Molinero. 2019. Assessing dual continuum method for multicomponent reactive transport. *Computers & Geosciences*. 130: 11-19.
5. Hyman, J. D., S. Karra, N. Makedonska, C. W. Gable, S. L. Painter, and H. S. Viswanathan 2015. "DFNWORKS: A discrete fracture network framework for modeling subsurface flow and transport". *Computers & Geosciences*, 84, 10-19.
6. Lichtner, P.C. (2000) Critique of Dual Continuum Formulations of Multicomponent Reactive Transport in Fractured Porous Media, Ed. Boris Faybishenko, Dynamics of Fluids in Fractured Rock, Geophysical Monograph 122, 281–298.
7. Lichtner, P.C. and S. Karra, 2014. Modeling multiscale-multiphase-multicomponent reactive flows in porous media: Application to CO₂ sequestration and enhanced geothermal energy using PFLOTRAN. *Computational Models for CO₂ Geo-Sequestration & Compressed Air Energy Storage*, CRC Press, 81-126.
8. Mariner, P. E., J. H. Lee, E. L. Hardin, F. D. Hansen, G. A. Freeze, A. S. Lord, B. Goldstein, and R. H. Price 2011. *Granite Disposal of U.S. High-Level Radioactive Waste*. SAND2011-6203. Sandia National Laboratories, Albuquerque, NM.
9. SKBF. 1983. Final storage of spent nuclear fuel - KBS-3. Volumes I - IV. Stockholm: Swedish Nuclear Fuel and Waste Management.
10. Stein, E. R., J. M. Frederick, G. E. Hammond, K. L. Kuhlmann, P. E. Mariner, and S. D. Sevougin 2017, April 9-13, 2017. *Modeling Coupled Reactive Flow Processes in Fractured Crystalline Rock*. Paper presented at the International High-Level Radioactive Waste Management Conference, Charlotte, NC.
11. Sudicky, E. A. and E. O. Frind 1982. CONTAMINANT TRANSPORT IN FRACTURED POROUS-MEDIA - ANALYTICAL SOLUTIONS FOR A SYSTEM OF PARALLEL FRACTURES. *Water Resources Research*, 18(6), 1634-1642.
12. Tang DH, Frind, EO and Sudicky EA, 1981. Contaminant transport in fracture porous media: analytical solution for a single fracture. *Water Resources Research*, 17(3), 555-564.